Molecular Therapy
Oncolytics
Original Article

Decreasing the Susceptibility of Malignant Cells to Infection Does Not Impact the Overall Efficacy of Myxoma Virus-Based Oncolytic Virotherapy

Erica B. Flores[1] and Eric Bartee[1]

[1]Department of Internal Medicine, Division of Molecular Medicine, University of New Mexico Health Sciences Center, Albuquerque, NM 87131, USA

Oncolytic virotherapy relies on the induction of anti-tumor immune responses to achieve therapeutic efficacy. The factors that influence the induction of these responses, however, are not well understood. To begin to address this lack of knowledge, we asked how decreasing the susceptibility of malignant cells to direct viral infection would impact the induction of immune responses and therapeutic efficacy caused by oncolytic myxoma virus treatment. To accomplish this, we used CRISPR-Cas9 genome editing to remove the essential sulfation enzyme N-deacetylase/N-sulfotransferase-1 from B16/F10 murine melanoma cells. This eliminates the negative cell surface charges associated with glycosaminoglycan sulfation, which reduces a cell's susceptibility to infection with the myxoma virus by ~3- to 10-fold. With the use of these cells as a model of reduced susceptibility to oncolytic infection, our data demonstrate that 3- to 10-fold reductions in *in vivo* infection do not hinder the ability of the oncolytic myxoma virus to induce anti-tumor immunity and do not lower the overall efficacy of localized treatment. Additionally, our data show that in mice bearing multiple distinct tumor masses, the choice to treat a less-susceptible tumor mass does not reduce the overall therapeutic impact against either the injected or noninjected lesion. Taken together, these data suggest that minor changes in the susceptibility of malignant cells to direct oncolytic infection do not necessarily influence the overall outcomes of treatment.

INTRODUCTION

Oncolytic virotherapy (OV) is a cancer treatment strategy based on the specific infection of malignant cells by tumor-tropic viruses. For many years, it was believed that the clinical efficacy of this treatment was mediated primarily through lytic destruction of directly infected tumor cells. More recently, however, it has become apparent that much of the tumor regression observed during OV is likely due to the viral induction of anti-tumor immune responses. Today, OV is therefore most-often viewed as a method to initiate or enhance T cell-mediated anti-tumor immunity.[1] Unfortunately, in contrast to the relatively well-understood process of direct lytic destruction, the factors that influence the ability of OV to induce these anti-tumor immune responses are not clearly defined. This lack of understanding is particularly problematic for OV, since, as with many immunotherapies, treatment often displays highly biphasic responses, with some patients displaying impressive tumor regressions, whereas others gain little to no benefit. Therefore, there is an urgent need to better understand the factors that influence and are likely to predict responsiveness to OV.

One factor that is frequently suggested to predict the efficacy of OV is the susceptibility of malignant cells to direct viral infection.[2] Indeed, the OV field has a long history of choosing both viral candidates and potential target malignancies based on the rate of tumor cell infectivity *in vitro*.[3–8] The theoretical rationale for this is relatively straightforward. Higher susceptibility of malignant cells should mean higher rates of total infection, which would likely translate into greater induction of anti-tumor immunity. However, although tumors that are totally resistant to viral infection are frequently found to be nonresponsive,[9] it is unclear how more subtle changes in susceptibility to infection might influence the outcomes of OV, particularly outcomes mediated primarily by anti-tumor immune responses.

We have recently demonstrated that the cellular protein N-deacetylase/N-sulfotransferase-1 (NDST1) plays a critical role in mediating the susceptibility of melanoma cells to infection with oncolytic myxoma virus (strain Lausanne) expressing green fluorescent protein (GFP) under regulation of the consensus poxviral synthetic early/late promoter (termed MYXV in this manuscript).[10] Loss of NDST1 prevents the addition of negatively charged sulfate groups onto cell-surface heparin chains.[11] Since these negatively charged sulfates play a key role in the initial electrostatic interaction between cells and infecting poxviral particles,[12–14] loss of NDST1 decreases the efficiency of MYXV binding and reduces the rate of viral infection by 3- to 10-fold. Since melanoma is highly susceptible to immunotherapies[15]and is therefore one of the most frequent target malignancies for OV,[16] we sought to advance on our previous observations by examining how this reduction in susceptibility to direct infection might influence the outcomes of MYXV-based treatment of melanomas.

Received 24 August 2020; accepted 20 October 2020;
https://doi.org/10.1016/j.omto.2020.10.011.

Correspondence: Eric Bartee, Department of Internal Medicine, Division of Molecular Medicine, Room 309A, Cancer Research Facility, University of New Mexico Health Sciences Center, Albuquerque, NM 87131, USA.
E-mail: ebartee@salud.unm.edu

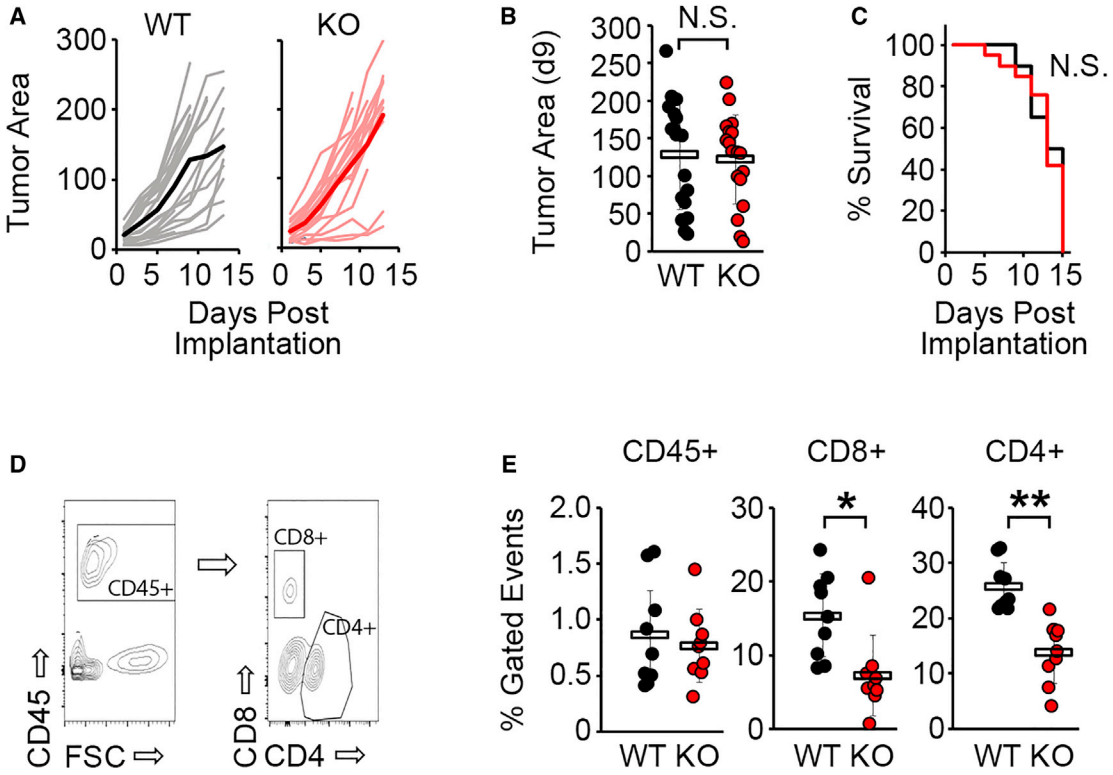

Figure 1. Loss of NDST1 Does Not Alter Melanoma Tumor Growth *In Vivo*

Tumors were established by injecting either NDST1^{+} (WT) or NDST1$^{-/-}$ (KO) B16/F10 cells subcutaneously into C57BL/6 mice. (A) Growth of individual tumors over time. Average tumor area of all tumors is marked by a darker line. (B) Average tumor area of all tumors 9 days after implantation (the day the first animal was euthanized). Significance was determined using Student's t test. (C) Overall survival of animals. (A–C) Data represent the summation of three independent experiments (WT n = 21, KO n = 21). Significance was determined using log-rank analysis. (D and E) Tumors from a subset of animals were excised 12 days after implantation and immune infiltration analyzed using flow cytometry. (D) Example of gating strategy used. (E) Quantitation of individual immune subsets within each excised tumor. (E) Data represent the summation of two independent experiments (WT n = 9, KO n = 9). Significance was determined using Student's t test (*$p < 0.05$, **$p < 0.01$; N.S., not significant).

RESULTS

Loss of NDST1 Reduces the Susceptibility of Melanoma Tumors to Infection with Oncolytic MYXV

Nontargeted informatics analysis has correlated NDST1 expression with poor prognosis in several forms of malignancy, including ovarian cancer and endometrial cancer.[17] Additionally, the enzyme has been previously reported to be highly expressed in many primary melanomas.[17–19] In order to support our use the NDST1-deficient B16/F10 cells as a model of altered susceptibility to MYXV infection, we therefore asked whether loss of this protein would impact melanoma growth in the absence of MYXV therapy. 4×10^5 NDST1^{+} (wild-type [WT]) or NDST1$^{-/-}$ (knockout [KO]) B16/F10 cells were injected subcutaneously (s.c.) into the left flank of syngeneic C57BL/6 mice. Once tumors became palpable (around 4 days after infection), tumor area was monitored every other day until tumors reached 15 mm in any direction, at which point, animals were euthanized, and intratumoral T cell infiltration was determined using flow cytometry. Consistent with loss of NDST1 not being a significant prognostic factor for melanoma, all mice injected with both WT (n = 20) and KO (n = 21) cells formed palpable tumor masses by 4 days postinjection (data not shown), and no quantitative or qualitative differences in tumor growth could be identified after their establishment (Figures 1A–1C). Similarly, both WT and KO tumors were infiltrated with comparable numbers of total CD45^{+} cells 14 days after implantation, although the makeup of this infiltration did differ between cohorts, with KO tumors displaying slightly reduced percentages of both CD8^{+} and CD4^{+} T cells (Figures 1D and 1E).

We have previously shown that loss of NDST1 reduces the binding of MYXV particles to the cell surface, which results in an ~3-fold decrease in their susceptibility to viral infection (Figures 2A and 2B).[10] To further validate our use of NDST1-deficient B16/F10 tumors as a model of reduced oncolytic infection, we next asked whether this reduced infectivity was maintained in NDST1-deficient tumors *in vivo*. Both WT and KO cells were injected s,c., into syngeneic animals and tumors allowed to establish until they reached ~25–30 mm^2. Tumors were then treated with a single injection of 1×10^7 foci-forming units (FFUs) of MYXV expressing GFP (vGFP) (Figure 2C). 24 h after viral treatment, tumors were excised and viral

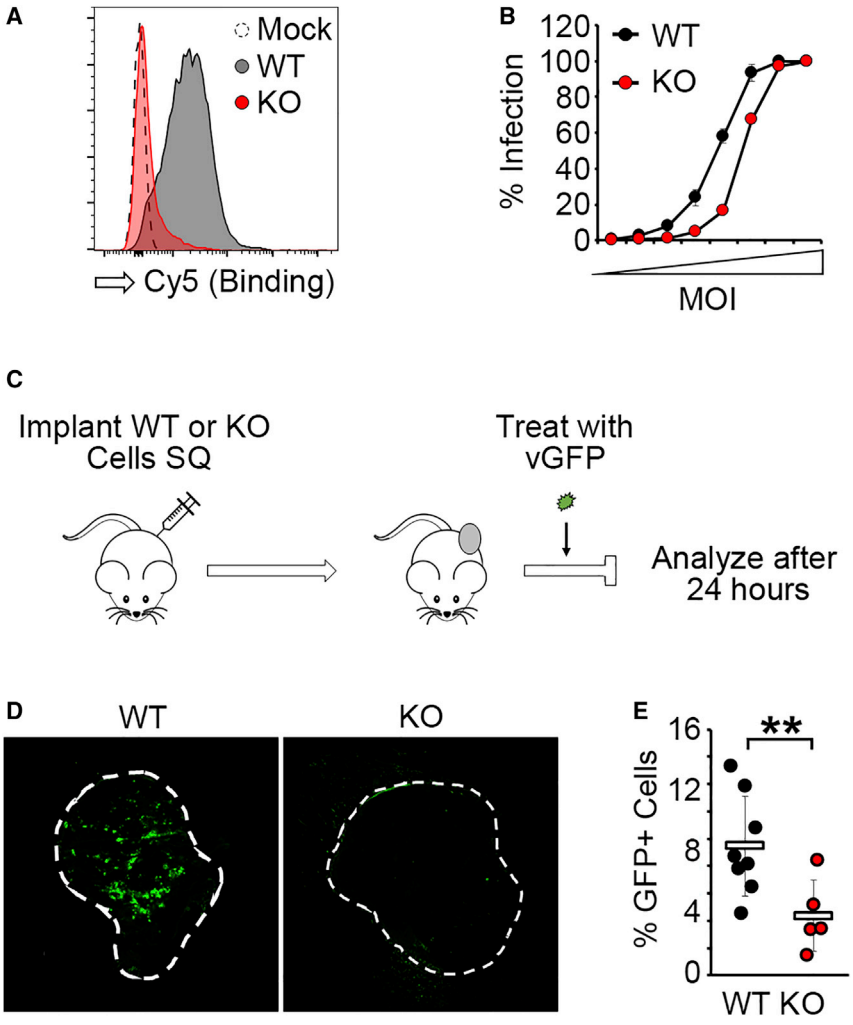

Figure 2. Tumors Lacking NDST1 Are Less Susceptible to MYXV Infection

(A) Either NDST1^{+} (WT) or NDST1$^{-/-}$ (KO) B16/F10 cells were incubated with Cy5-labeled MYXV particles. Direct binding of viral particles to the cell surface was then measured by flow cytometry. (B) WT or KO B16/F10 cells were infected with various MOIs of MYXV, ranging from 0.001 to 3. The rate of viral infection as then determined by quantitating the percent of GFP^{+} cells 24 h after infection using flow cytometry. Data are representative of three individual experiments. (C–E) WT or KO tumors of ~25–35 mm^2 were treated with a single intratumoral infection of 1×10^7 FFU of MYXV (C). Tumors were excised 24 h after treatment. (D) Visualization of GFP^{+} region of infection in 8 μM sections of snap-frozen tumors. (E) Quantitation of the percent of GFP^{+} cells in each tumor analyzed using flow cytometry. (D and E) Data represent the summation of two independent experiments (WT n = 8, KO n = 5). Significance was determined using Student's t test (**p < 0.01). SQ, subcutaneous.

infection was assessed either by visual examination of tumor sections (Figure 2D) or flow cytometric quantitation of GFP^{+} cells (Figure 2E). Consistent with our previous *in vitro* results, these *in vivo* results demonstrated that NDST1-deficient tumors displayed significantly reduced viral infection following treatment with oncolytic MYXV. Taken together, these data indicate that loss of NDST1 does not alter the inherent growth properties of B16/F10 tumors but does reduce the susceptibility of these tumors to oncolytic MYXV infection by ~3- to 10-fold.

Decreased Susceptibility to Infection Does Not Alter MYXV-Mediated Induction of Anti-tumor Immunity

As with many oncolytic viruses, MYXV achieves its efficacy primarily by enhancing anti-tumor immunity.[9,20,21] We have recently demonstrated that the induction of these immune responses is highly influenced by large changes in the initial viral dose (>2 logs) and absolutely requires viral replication.[22] We therefore wished to determine how the much smaller changes in susceptibility to infection induced by loss of NDST1 would influence the generation of anti-tumor immunity following MYXV treatment. WT and KO tumors were established in syngeneic C57BL/6 animals and subsequently treated with three doses of 1×10^7 FFU of MYXV over 5 days. 24 h after the final viral injection, tumors were excised, and the overall viral burden, as well as the localized immune response, was analyzed using flow cytometry (Figure 3A). Consistent with loss of NDST1 inhibiting MYXV infection, we observed a significant reduction (~17-fold, p = 0.006) in total viral burden in KO tumors compared to WT tumors (Figure 3B). In contrast, both WT and KO tumors treated with MYXV displayed similarly increased levels of adaptive immune activity compared to mock-treated tumors, including statistically indistinguishable overall levels of both CD8^{+} and CD4^{+} T cells (Figure 3C). Interestingly, KO tumors appeared to display an increased level of innate immune activity after viral treatment, characterized primarily by an enhanced number of tumor-associated macrophages (MACS).

Since MYXV achieves therapeutic efficacy through the induction of anti-tumor immunity, we next wished to determine whether the similar induction of this immunity in KO tumors would be sufficient to fully recapitulate MYXV-based treatment even with reduced levels of direct viral infection. To test this, 4×10^5 WT or KO cells were injected into the left flank of C57BL/6 mice as above. Once tumors had reached ~25 mm^2, both WT and KO tumor-bearing mice were randomly separated into two additional cohorts and treated with three doses of either saline or 1×10^7 FFU of MYXV. Tumor growth on each mouse was then monitored until tumors reached 15 mm in any direction, at which point, the animal was humanely euthanized (Figure 4A). In striking contrast to their different susceptibilities to viral infection, both WT and KO tumors treated with oncolytic

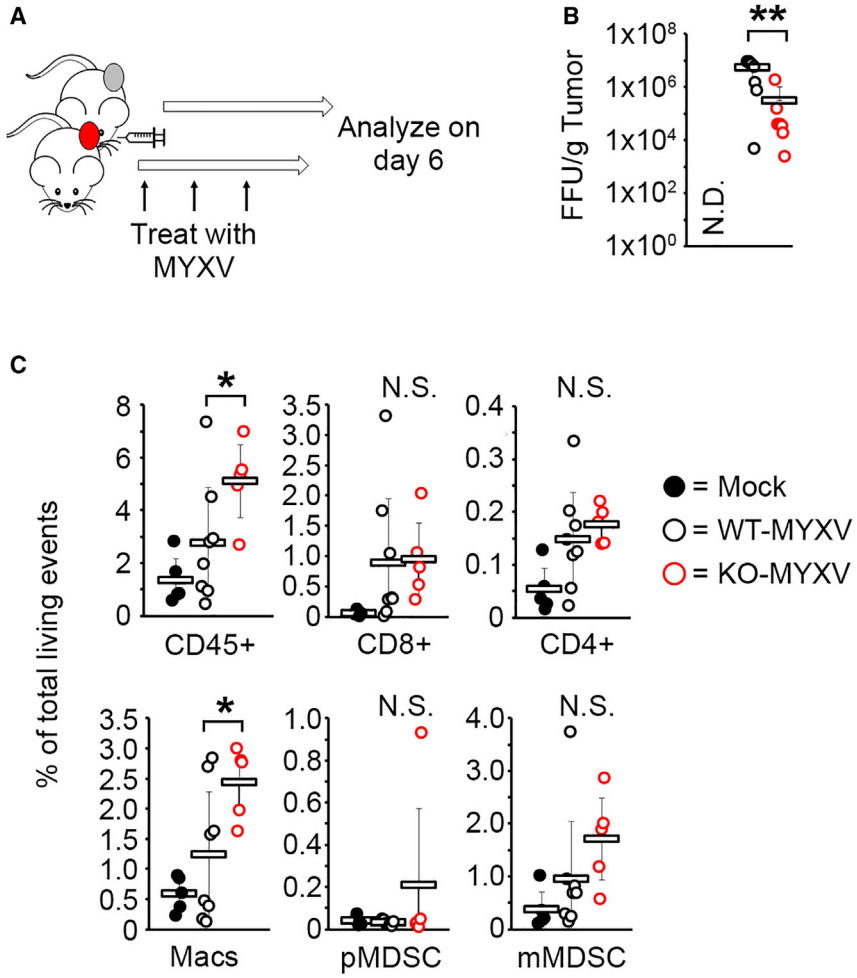

Figure 3. Reduced Direct Viral Infection Does Not Alter the Induction of Intratumoral Immune Responses

(A) Schematic of experimental design. C57BL/6 mice were injected subcutaneously with either NDST1^{+} (WT) or NDST1$^{-/-}$ (KO) B16/F10 cells and tumors allowed to establish until they reached ~25 mm^2. Tumors were then either mock treated or treated with three injections of 1 × 10^7 FFU of MYXV over 5 days. On the 6th day, tumors were excised and analyzed. (B) Number of infectious viral particles in treated tumors. Data are normalized to tumor weight and represent the summation of two independent experiments (WT n = 8, KO n = 7). Significance was determined using Student's t test (**p < 0.01). (C) Quantitation of individual immune subsets within the indicated tumors. All data are pregated on single/living events. Data are representative of two independent experiments (mock n = 6, WT n = 8, KO n = 5). Significance was determined using Student's t test (*p < 0.05).

MYXV displayed statistically indistinguishable delays in tumor progression compared to untreated controls (Figures 4B and 4C), and this delay resulted in virtually identical improvements in overall animal survival (Figure 4D). To confirm that this delayed tumor growth was purely the result of virally induced anti-tumor immunity, we conducted a similar experiment in T cell-deficient non-obese diabetic (NOD)/severe combined immunodeficiency (SCID) mice. Following treatment, individual tumor growth was monitored for 10 days, at which point, tumors were harvested, and total viral load as well as tumor mass analyzed (Figure 5A). Consistent with KO tumors having an inherently reduced susceptibility to MYXV infection, we observed that even in NOD/SCID mice, KO tumors treated with virus displayed lower total viral loads than WT tumors 10 days after treatment (Figure 5B). In contrast to our previous results in immune-competent mice, however, in the absence of adaptive immunity, we observed that MYXV-treated tumors were unable to meaningfully delay the growth of either WT or KO tumors (Figures 5C–5E), suggesting that the efficacy observed in C57BL/6 mice was purely the result of virally induced anti-tumor immunity. Taken together, these data suggest that minor reductions in the susceptibility of tumor cells to viral infection do not impact the initiation of immune responses within treated tumors and do not alter therapeutic efficacy in models where this efficacy is mediated primarily by anti-tumor immunity.

Treatment of a Less Susceptible Lesion Does Not Alter Efficacy against Disseminated Disease

Most OV treatments, including the US Food and Drug Administration (FDA)-approved oncolytic virus Imlygic, are delivered locally via direct intratumoral injections. In stark contrast, the vast majority of cancer patients in need of immunotherapy present with a highly disseminated disease. This can force the treating physician to choose which lesion(s) should be directly treated with the oncolytic virus. Critically, it has long been known that significant heterogeneity exists between distinct tumor masses in disseminated disease;[23,24] however, there is currently little understanding of how the choice of which tumor mass to treat impacts overall therapeutic efficacy. We therefore asked whether the choice to treat a less-susceptible tumor mass on a mouse bearing disseminated lesions would hinder the overall efficacy of treatment. In order to address this issue, we first generated B16/F10 cells that lacked both NDST1 and programmed death ligand 1 (PDL1) (Figure S1). The deletion of PDL1 increases the susceptibility of tumors to immunotherapy, enhancing our ability to detect efficacy in contralateral models.[25] Immune-competent C57BL/6 mice were then injected on the right side with a bolus of single PDL1$^{-/-}$ deficient cells and on the left side with a second bolus of either PDL1$^{-/-}$ deficient cells (KO/KO) or a bolus of double KO (DKO) NDST1$^{-/-}$/PDL1$^{-/-}$ cells (KO/DKO) (Figure 6A). Once both tumors had reached ~25 mm^2, mice were treated by injecting three doses of 1 × 10^7 FFU of MYXV into the tumor on the left side. Tumors on the right side of the animal were left untreated. Growth of both tumors was then

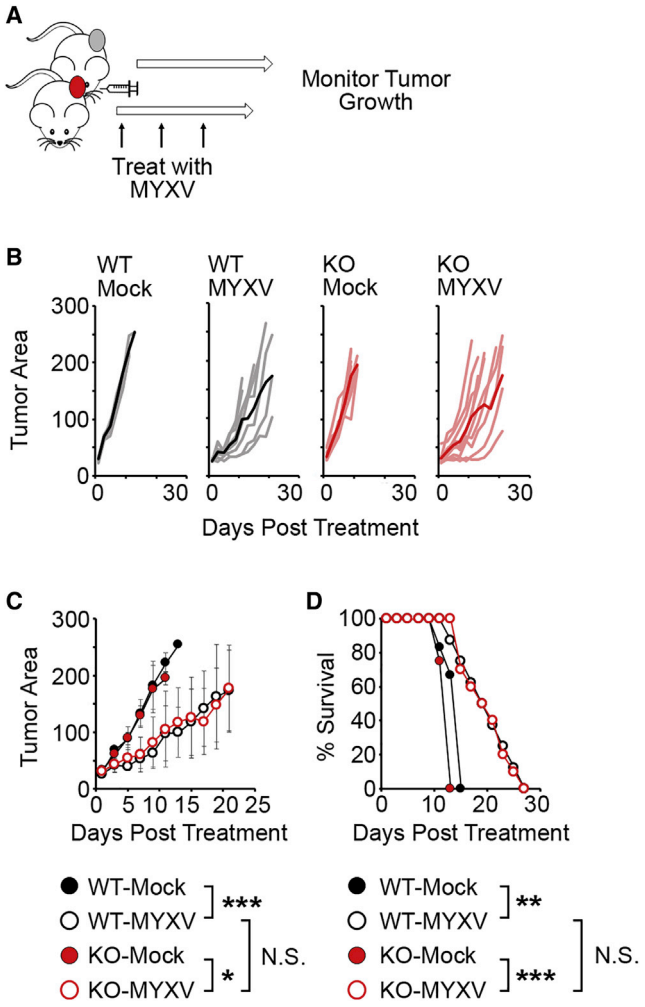

Figure 4. Reduced Direct Viral Infection Does Not Inhibit the Overall Efficacy of MYXV Therapy

(A) Schematic of experimental design. C57BL/6 mice were injected subcutaneously with either NDST1^{+} (WT) or NDST1$^{-/-}$ (KO) B16/F10 cells and tumors allowed to establish until they reached ~25 mm^2. Tumors were then either mock treated or treated with three injections of 1 × 10^7 FFU of MYXV over 5 days. (B) Growth of individual tumors over time. Average tumor area of all tumors is marked by a darker line. (C) Average tumor area of all tumors. Significance was determined at day 11 post-treatment using Student's t test (*$p < 0.05$, ***$p < 0.001$). (D) Overall survival of animals. Significance was determined using log-rank test (**$p < 0.01$, ***$p < 0.001$). (B–D) Data represent the summation of two independent experiments (WT mock n = 6, KO mock n = 8, WT MYXV n = 8, KO MYXV n = 10).

monitored until the animal's total tumor burden exceeded 400 mm^2, at which point, the animal was humanely euthanized (Figures 6B and 6C). Although significant variation was observed in these experiments, due to the complex model design, the results suggested that MYXV treatment significantly improved overall survival primarily by delaying tumor growth in directly injected lesions. Critically, however, no significant differences in either the delay of tumor growth or the improved overall survival were observed between mice that were injected into a fully susceptible or a less-susceptible tumor mass. These data suggest that treatment of a lesion that displays reduced susceptibility to directly oncolytic infection does not compromise overall therapeutic efficacy as long as the induction of anti-tumor immunity remains robust.

DISCUSSION

Here, we have examined how minor changes to the susceptibility of malignant cells to direct infection with oncolytic MYXV impact the overall efficacy of OV. To achieve this reduced susceptibility, we used a B16/F10 melanoma model lacking the essential sulfation enzyme NDST1, which our lab has previously shown reduces susceptibility of these cells to MYXV infection by ~3- to 10-fold (Figure 2).[10] Interestingly, whereas nonspecific informatics analysis has suggested that NDST1 might represent a negative prognostic factor in both ovarian and endometrial cancer,[17] B16/F10 melanomas lacking this enzyme did not display any altered growth *in vivo* (Figure 1). These tumors did, however, display a slight reduction in overall immune activity at late time points postimplantation (Figure 1). This is consistent with previous reports that NDST1, expressed in the vascular endothelium, can play a role in leukocyte adhesion.[26] Although there does not appear to be any evidence that this minor change in base-line immune activity influenced the results of our present study, it does suggest that future work examining the overall role of NDST1 in tumor immunity and possibly immunotherapy could be warranted.

In contrast to their similar overall growth properties, tumors derived from NDST1$^{-/-}$ cells displayed a pronounced reduction in viral infection following direct intratumoral injection (Figure 3). This reduction corresponded to an ~2- to 3-fold reduction in the number of infected cells 24 h after injection (Figure 2D) and a significantly more pronounced ~15-fold reduction in the total infectious virus 6 days after injection (Figure 3B). Interestingly, this trend toward an increasing discrepancy over time is in direct contrast to previous reports in which highly variable initial doses of the oncolytic virus eventually resulted in completely normalized overall viral burdens.[22] Critically, in both the current and previous works, the immune responses resulting from viral injection appear to correlate with the initial oncolytic infection and not with the subsequent overall viral load (Figure 3). Both works therefore appear to support the overall concept that the induction of immune responses following MYXV-based OV is durably programmed by events that occur extremely early after treatment. The exact nature of these events, however, has not yet been elucidated.

In terms of localized therapeutic efficacy, our work suggests that tumors with reduced susceptibility to viral infection might not display worse outcomes following oncolytic treatment (Figure 4). Although the data supporting this argument are quite clear in our specific model, there are numerous caveats that must be taken into account. First, the reduction in viral infection resulting from loss of NDST1 is relatively minor (~3- to 10-fold). Based on the small magnitude of this reduction, it is possible that tumors that display much greater reductions in susceptibility to infection (i.e., >10-fold) would indeed

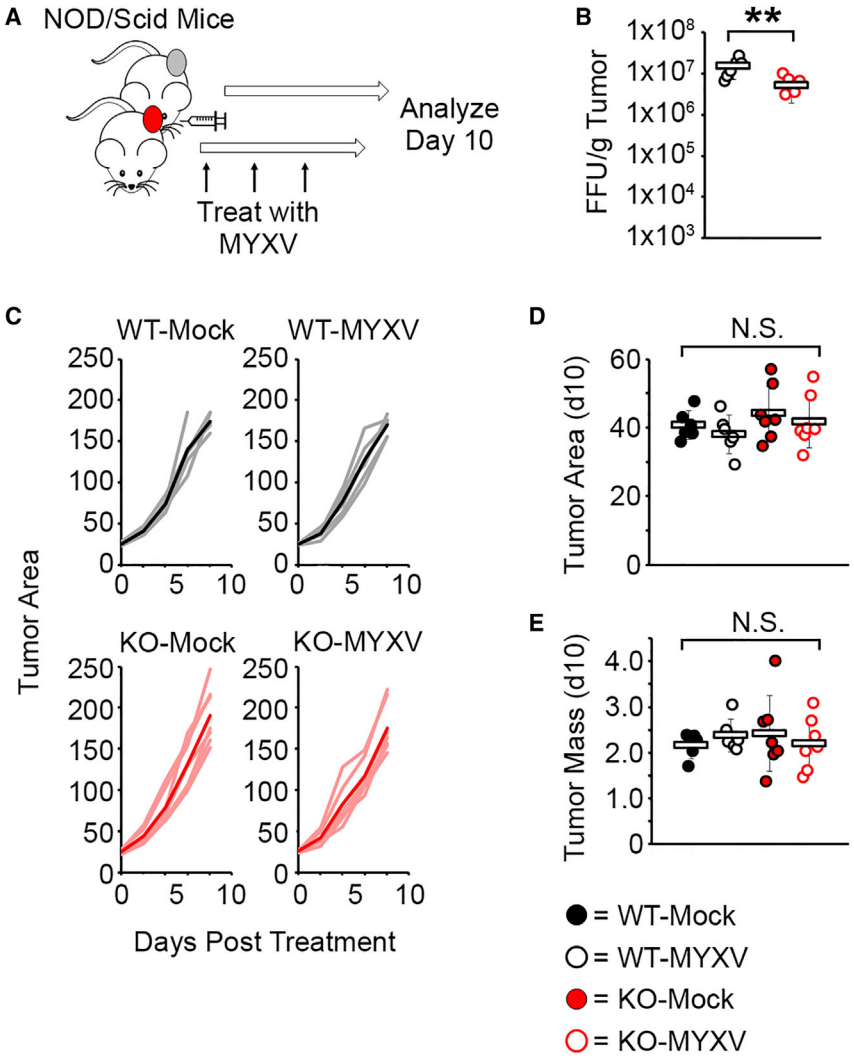

Figure 5. Efficacy of MYXV Treatment Is Based Primarily on Anti-tumor Immunity

(A) Schematic of experimental design. NOD/SCID mice were injected subcutaneously with either NDST1^{+} (WT) or NDST1$^{-/-}$ (KO) B16/F10 cells and tumors allowed to establish until they reached ~25 mm^2. Tumors were then either mock treated or treated with three injections of 1 × 10^7 FFU of MYXV over 5 days. 10 days after the initiation of treatment, tumors were harvested and analyzed for viral burden. (B) Number of infectious viral particles in treated tumors. Data are normalized to tumor weight. Significance was determined using Student's t test (**p < 0.01). (C) Growth of individual tumors over time. Average tumor area of all tumors is marked by a darker line. (D) Average tumor area 10 days after the initiation of treatment. Significance was determined using Student's t test. (E) Average tumor mass 10 days after the initiation of treatment. Significance was determined using Student's t test (WT mock n = 6, KO mock n = 6, WT MYXV n = 7, KO MYXV n = 7).

have poorer therapeutic outcomes. If this is true, it would be interesting to determine whether this decreased efficacy followed a dose-response-type curve or instead displayed a critical threshold that must be met. Although our current work does not address this specific issue, previous work has suggested that the induction of anti-tumor immunity by varying initial doses of oncolytic MYXV appears to be based primarily on the surpassing of a critical threshold.[22] Second, it is unclear whether the specific nature of the change causing reduced susceptibility to infection is critical in determining the immunological outcomes. For example, loss of NDST1 inhibits MYXV infection by preventing viral adsorption to the cell surface. Other molecular events, however, have also been shown to partially reduce MYXV infectivity at later stages of the viral replication cycle.[27,28] Whether loss of overall infectivity at a different stage of viral replication might have a different impact on therapeutic efficacy therefore remains unclear. Third, our NDST1-deficient model recreates an equal reduction in susceptibility to viral infection in all malignant cells within a single tumor lesion. However, most clinical tumors display significant intratumoral heterogeneity.[29,30] It is therefore likely that a single tumor mass will contain some tumor cells with high susceptibility to infection and others with much lower susceptibility. How this form of partially reduced susceptibility to infection might influence OV remains to be determined. Finally, it is noted that the overall efficacy of treatment with unmodified MYXV is not clinically impressive in the B16/F10 model used in our studies. In contrast, most clinically effective oncolytic treatments are based on therapeutic viruses expressing one or more exogenous transgenes, and expression of these transgenes is likely to be significantly impacted by altered rates of viral infection. Unfortunately, since our current studies were conducted with a virus that does not express such transgenes, we are unable to predict how altered viral infectivity might influence expression of therapeutic transgenes and the subsequent efficacy of viruses that express them. Additional work on this question is therefore required to fully understand the application of our results into clinical practice.

Lastly, OV is most often delivered through localized intratumoral injections. Many patients receiving this therapy, however, are likely to present with more lesions than can be directly injected. This means that a treating physician must choose which tumor masses to treat and which to leave noninjected. Critically, there is currently little evidence on how the choice of which lesion to inject might influence overall therapeutic efficacy. In this context, our work suggests that the choice to treat a slightly less-susceptible tumor mass does not hinder the overall systemic efficacy of localized OV (Figure 6). This result is likely due to the efficacy of MYXV-based OV being mediated primarily through

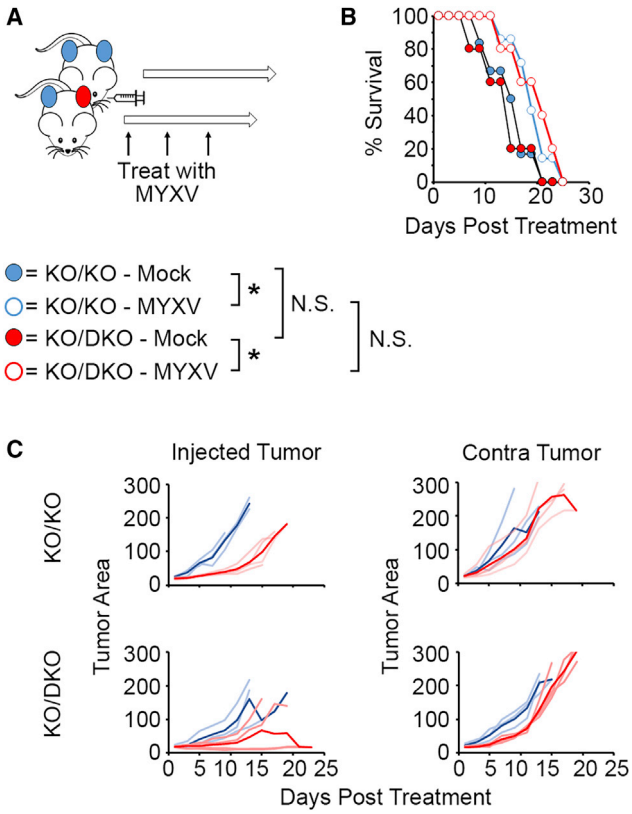

Figure 6. Treatment of a Less-Susceptible Tumor Mass Does Not Reduce Overall Systemic Efficacy during Localized OV

(A) Schematic of experimental design. C57BL/6 mice were injected on each flank with either PDL1$^{-/-}$ (KO/KO, blue) or PDL1$^{-/-}$/NDST1$^{-/-}$ (KO/DKO, red) cells, as indicated, and tumors allowed to establish until both tumors reached ~25 mm^2. The tumor on the left anatomical flank was then either mock treated or treated with three injections of 1 × 10^7 FFU of MYXV over 5 days. Tumors on the right flank were left untreated. Growth of both tumors was then monitored, and mice euthanized with their total tumor burden exceeded 400 mm^2. (B) Overall survival of animals. Significance was determined using the log-rank test (*$p < 0.05$). (C) Average area of both injected and noninjected tumors from all cohorts. (B and C) Data represent the summation of two independent experiments (KO/KO mock n = 6, KO/DKO mock n = 5, KO/KO MYXV n = 7, KO/DKO MYXV n = 5).

the induction of abscopal immunity. For other oncolytic viruses that have more potent, direct lytic capacity, the choice of which tumor to treat might play a more important role. Regardless, this is a potentially critical line of study that certainly bears further examination.

In conclusion, our data suggest that whereas susceptibility of malignant cells to viral infection might be a critical factor in determining the efficacy of OV in some settings, minor decreases in the rates of tumor infectability do not always preclude successful treatment.

MATERIALS AND METHODS

Reagents and Viruses

MYXV has been previously described.[31] Unless otherwise noted, all viral infections were carried out using this GFP expressing MYXV and were conducted by inoculating cells with the indicated viral multiplicity of infection (MOI) for 1 h and subsequently replacing inoculum with fresh growth media. B16/F10 murine melanoma cells lacking NDST1 (KO) due to CRISPR-Cas9 genome editing, as well as relevant control cells, have been previously described.[10] Cells were maintained in Dulbecco's modified Eagle's medium (DMEM; Mediatech, Manassas, VA, USA), supplemented with 10% fetal bovine serum (VWR, Radnor, PA, USA) and 100 U/ml penicillin-streptomycin (Mediatech, Manassas, VA, USA).

Generation of NDST1$^{-/-}$/PDL1$^{-/-}$ B16/F10 Cells

A B16/F10 cell line, which is incapable of expressing PDL1 due to CRISPR-Cas9 genomic editing, has been previously described.[25] To generate doubly deleted NDST1$^{-/-}$/PDL1$^{-/-}$ cells, the existing PDL1-deficient cells were transfected with a plasmid encoding the Cas9 enzyme and a NDST1-specific guide RNA (gRNA; sequence [seq] 5′-AAGCCACGGCGGTACCGGGC-3′) (pSpCas9BB-24-2A-Puro; GenScript, Piscataway, NJ). A matched PDL1$^{-/-}$/NDST1^{+} cell line was also created using a scrambled gRNA (seq 5′-GC GAGGTCTTCGGCTCCGCG-3′). 48 h after transfection, cells were transferred to media containing 1 μg/mL puromycin for 1 week to select for transfected cells. Cells were then removed from selective media, and single cells were expanded as individual clonal lines. Two original single NDST1 lines were examined for the construction of this DKO line. *In vivo* studies were conducted with line #1.

In Vivo Animal Studies

6- to 8-week-old C57BL/6 mice (Charles River Laboratories, Raleigh, NC, USA) were injected s.c. with 4 × 10^5 B16/F10 cells on either the left flank or both flanks. Tumors were left to establish until they reached a size of ~2 5mm^2. For tumor establishment studies, no tumors were excluded from analysis. For all other studies, tumors displaying "abnormal" size following establishment (based on individual investigator assessment) were removed from the experiment prior to cohort separation. Following removal of abnormal tumor-bearing mice, animals were randomly binned into the indicated cohorts and treated with MYXV. All data from treated mice are shown in the resulting figures. Viral treatment consisted of three intratumoral injections of either saline or MYXV (1 × 10^7 total FFU in 50 μL phosphate-buffered saline [PBS]) on experimental days 1, 3, and 5. For survival studies, tumor area was monitored using calipers, and mice were euthanized when tumors reached predetermined criteria (15 mm in any direction for single tumor experiments and a total tumor burden of 400 mm^2 for contralateral experiments). All experiments were conducted in accordance with the Institutional Animal Care and Use Committees of both the Medical University of South Carolina and the University of New Mexico Health Sciences Center.

Tumor Immune Analysis

After euthanasia, tumors were surgically harvested and disassociated into single cells over a 40-μM mesh filter. Single cell suspensions were then incubated with the indicated antibodies, washed with PBS, and stained with the LIVE/DEAD Fixable Far Red Dead Cell Stain Kit

(Invitrogen, Carlsbad, CA) using standard flow cytometry methodologies. Samples were then analyzed on a BD FACSVerse cytometer (BD Biosciences, San Jose, CA, USA). All analyses shown are pregated on single, viable events. Immune populations were defined as follows: $CD8^+$ T cells ($CD45^+/CD3^+/CD8^+/CD4^-$), conventional $CD4^+$ T cells (T_{con}; $CD45^+/CD3^+/CD8^-/CD4^+$), MACS ($CD45^+/F4/80^+$),[32] plasmacytoid myeloid-derived suppressor cells (pMDSCs; $CD45^+/F4/80^-/Ly6C^{hi}/Ly6G^-$), and monocytic MDSCs (mMDSCs; $CD45^+/F4/80^-/Ly6C^{lo}/Ly6G^+$).[33]

Imaging of Viral Infections within Tumors

After euthanasia, tumors were surgically harvested and snap frozen in optimal cutting temperature (OCT) compound (Scigen Scientific, Gardena, CA). Frozen tissue was then sectioned into 8 μM sections and each section placed on a glass slide. GFP^+ regions of infection were then imaged on a Zeiss LSM 800 Airyscan confocal microscope and images stitched together using Adobe Photoshop software. Images have been contrast enhanced after collection to enhance visualization of foci. All images were treated identically during processing.

Quantitation of Infectious Virus in Tumors

After euthanasia, tumors were surgically harvested, weighed, and then disassociated into single cells over a 40-μM mesh filter. 10% of the resulting cell pellet was then placed in a new tube and flash frozen. Virus was subsequently released from cell pellets by repeated cycles of freeze thawing and sonication. Amount of infectious virus in each sample was determined using standard viral foci-forming assays on BSC40 cells. All viral titer data are back normalized to total tumor weight and presented as FFUs per gram of tumor.

SUPPLEMENTAL INFORMATION

Supplemental Information can be found online at https://doi.org/10.1016/j.omto.2020.10.011.

ACKNOWLEDGMENTS

We would like to thank Dr. Paula Traktman for valuable discussions concerning the overall project. This work was funded by the following grants to EB: R01CA194090 and R21AI142387 from the NIH and RSG-17-047-01-MPC from the American Cancer Society.

AUTHOR CONTRIBUTIONS

E.B.F. conducted experiments and analyzed data. E.B. oversaw the project, obtained funding, and wrote the manuscript.

DECLARATION OF INTERESTS

The authors declare no competing interests.

REFERENCES

1. Melcher, A., Parato, K., Rooney, C.M., and Bell, J.C. (2011). Thunder and lightning: immunotherapy and oncolytic viruses collide. Mol. Ther. *19*, 1008–1016.

2. Mahasa, K.J., Eladdadi, A., de Pillis, L., and Ouifki, R. (2017). Oncolytic potency and reduced virus tumor-specificity in oncolytic virotherapy. A mathematical modelling approach. PLoS ONE *12*, e0184347.

3. Nichols, A.C., Yoo, J., Um, S., Mundi, N., Palma, D.A., Fung, K., Macneil, S.D., Koropatnick, J., Mymryk, J.S., and Barrett, J.W. (2014). Vaccinia virus outperforms a panel of other poxviruses as a potent oncolytic agent for the control of head and neck squamous cell carcinoma cell lines. Intervirology *57*, 17–22.

4. Kuhn, I., Harden, P., Bauzon, M., Chartier, C., Nye, J., Thorne, S., Reid, T., Ni, S., Lieber, A., Fisher, K., et al. (2008). Directed evolution generates a novel oncolytic virus for the treatment of colon cancer. PLoS ONE *3*, e2409.

5. Kuhn, I., Bauzon, M., Green, N., Seymour, L., Fisher, K., and Hermiston, T. (2016). OvAd1, a Novel, Potent, and Selective Chimeric Oncolytic Virus Developed for Ovarian Cancer by 3D-Directed Evolution. Mol. Ther. Oncolytics *4*, 55–66.

6. Garijo, R., Hernández-Alonso, P., Rivas, C., Diallo, J.S., and Sanjuán, R. (2014). Experimental evolution of an oncolytic vesicular stomatitis virus with increased selectivity for p53-deficient cells. PLoS ONE *9*, e102365.

7. Seegers, S.L., Frasier, C., Greene, S., Nesmelova, I.V., and Grdzelishvili, V.Z. (2020). Experimental Evolution Generates Novel Oncolytic Vesicular Stomatitis Viruses with Improved Replication in Virus-Resistant Pancreatic Cancer Cells. J. Virol. *94*, e01643-19.

8. McKenzie, B.A., Zemp, F.J., Pisklakova, A., Narendran, A., McFadden, G., Lun, X., Kenchappa, R.S., Kurz, E.U., and Forsyth, P.A. (2015). In vitro screen of a small molecule inhibitor drug library identifies multiple compounds that synergize with oncolytic myxoma virus against human brain tumor-initiating cells. Neuro-oncol. *17*, 1086–1094.

9. Bartee, E., Bartee, M.Y., Bogen, B., and Yu, X.Z. (2016). Systemic therapy with oncolytic myxoma virus cures established residual multiple myeloma in mice. Mol. Ther. Oncolytics *3*, 16032.

10. Flores, E.B., Bartee, M.Y., and Bartee, E. (2020). Reduced cellular binding affinity has profoundly different impacts on the spread of distinct poxviruses. PLoS ONE *15*, e0231977.

11. Dou, W., Xu, Y., Pagadala, V., Pedersen, L.C., and Liu, J. (2015). Role of Deacetylase Activity of N-Deacetylase/N-Sulfotransferase 1 in Forming N-Sulfated Domain in Heparan Sulfate. J. Biol. Chem. *290*, 20427–20437.

12. Chung, C.S., Hsiao, J.C., Chang, Y.S., and Chang, W. (1998). A27L protein mediates vaccinia virus interaction with cell surface heparan sulfate. J. Virol. *72*, 1577–1585.

13. Ho, Y., Hsiao, J.C., Yang, M.H., Chung, C.S., Peng, Y.C., Lin, T.H., Chang, W., and Tzou, D.L. (2005). The oligomeric structure of vaccinia viral envelope protein A27L is essential for binding to heparin and heparan sulfates on cell surfaces: a structural and functional approach using site-specific mutagenesis. J. Mol. Biol. *349*, 1060–1071.

14. Shih, P.C., Yang, M.S., Lin, S.C., Ho, Y., Hsiao, J.C., Wang, D.R., Yu, S.S., Chang, W., and Tzou, D.L. (2009). A turn-like structure "KKPE" segment mediates the specific binding of viral protein A27 to heparin and heparan sulfate on cell surfaces. J. Biol. Chem. *284*, 36535–36546.

15. Garbe, C., Eigentler, T.K., Keilholz, U., Hauschild, A., and Kirkwood, J.M. (2011). Systematic review of medical treatment in melanoma: current status and future prospects. Oncologist *16*, 5–24.

16. Raedler, L. (2016). Talimogene laherparepvec (Imlygic) for unresectable melanoma. Med. Lett. Drugs Ther. *58*, 8–9.

17. Uhlén, M., Björling, E., Agaton, C., Szigyarto, C.A., Amini, B., Andersen, E., Andersson, A.C., Angelidou, P., Asplund, A., Asplund, C., et al. (2005). A human protein atlas for normal and cancer tissues based on antibody proteomics. Mol. Cell. Proteomics *4*, 1920–1932.

18. Uhlén, M., Fagerberg, L., Hallström, B.M., Lindskog, C., Oksvold, P., Mardinoglu, A., Sivertsson, Å., Kampf, C., Sjöstedt, E., Asplund, A., et al. (2015). Proteomics. Tissue-based map of the human proteome. Science *347*, 1260419.

19. Uhlen, M., Zhang, C., Lee, S., Sjöstedt, E., Fagerberg, L., Bidkhori, G., Benfeitas, R., Arif, M., Liu, Z., Edfors, F., et al. (2017). A pathology atlas of the human cancer transcriptome. Science *357*, eaan2507.

20. Ogbomo, H., Zemp, F.J., Lun, X., Zhang, J., Stack, D., Rahman, M.M., McFadden, G., Mody, C.H., and Forsyth, P.A. (2013). Myxoma virus infection promotes NK lysis of malignant gliomas in vitro and in vivo. PLoS ONE *8*, e66825.

21. Wennier, S.T., Liu, J., Li, S., Rahman, M.M., Mona, M., and McFadden, G. (2012). Myxoma virus sensitizes cancer cells to gemcitabine and is an effective oncolytic virotherapeutic in models of disseminated pancreatic cancer. Mol. Ther. *20*, 759–768.

22. Flores, E.B., Aksoy, B.A., and Bartee, E. (2020). Initial dose of oncolytic myxoma virus programs durable antitumor immunity independent of in vivo viral replication. J. Immunother. Cancer *8*, e000804.

23. Fidler, I.J., and Hart, I.R. (1981). The origin of metastatic heterogeneity in tumors. Eur. J. Cancer *17*, 487–494.

24. Hart, I.R., and Fidler, I.J. (1981). The implications of tumor heterogeneity for studies on the biology of cancer metastasis. Biochim. Biophys. Acta *651*, 37–50.

25. Bartee, M.Y., Dunlap, K.M., and Bartee, E. (2017). Tumor-Localized Secretion of Soluble PD1 Enhances Oncolytic Virotherapy. Cancer Res. *77*, 2952–2963.

26. Wang, L., Fuster, M., Sriramarao, P., and Esko, J.D. (2005). Endothelial heparan sulfate deficiency impairs L-selectin- and chemokine-mediated neutrophil trafficking during inflammatory responses. Nat. Immunol. *6*, 902–910.

27. Bartee, E., Mohamed, M.R., Lopez, M.C., Baker, H.V., and McFadden, G. (2009). The addition of tumor necrosis factor plus beta interferon induces a novel synergistic antiviral state against poxviruses in primary human fibroblasts. J. Virol. *83*, 498–511.

28. Wang, F., Gao, X., Barrett, J.W., Shao, Q., Bartee, E., Mohamed, M.R., Rahman, M., Werden, S., Irvine, T., Cao, J., et al. (2008). RIG-I mediates the co-induction of tumor necrosis factor and type I interferon elicited by myxoma virus in primary human macrophages. PLoS Pathog. *4*, e1000099.

29. Pribluda, A., de la Cruz, C.C., and Jackson, E.L. (2015). Intratumoral Heterogeneity: From Diversity Comes Resistance. Clin. Cancer Res. *21*, 2916–2923.

30. Renovanz, M., and Kim, E.L. (2014). Intratumoral heterogeneity, its contribution to therapy resistance and methodological caveats to assessment. Front. Oncol. *4*, 142.

31. Johnston, J.B., Barrett, J.W., Chang, W., Chung, C.S., Zeng, W., Masters, J., Mann, M., Wang, F., Cao, J., and McFadden, G. (2003). Role of the serine-threonine kinase PAK-1 in myxoma virus replication. J. Virol. *77*, 5877–5888.

32. Broz, M.L., Binnewies, M., Boldajipour, B., Nelson, A.E., Pollack, J.L., Erle, D.J., Barczak, A., Rosenblum, M.D., Daud, A., Barber, D.L., et al. (2014). Dissecting the tumor myeloid compartment reveals rare activating antigen-presenting cells critical for T cell immunity. Cancer Cell *26*, 638–652.

33. Bronte, V., Brandau, S., Chen, S.H., Colombo, M.P., Frey, A.B., Greten, T.F., Mandruzzato, S., Murray, P.J., Ochoa, A., Ostrand-Rosenberg, S., et al. (2016). Recommendations for myeloid-derived suppressor cell nomenclature and characterization standards. Nat. Commun. *7*, 12150.